PRAMANA — journal of physics
© Indian Academy of Sciences
Vol. 77, No. 5
November 2011
pp. 949–957

Collisionless stopping of electron current in an inhomogeneous electron magnetohydrodynamics plasma

AMITA DAS*, SHARAD K YADAV, PREDHIMAN KAW and SUDIP SENGUPTA
Institute for Plasma Research, Bhat, Gandhinagar 382 428, India
*Corresponding author. E-mail: amita@ipr.res.in

Abstract. A brief review of a recent work on a novel collisionless scheme for stopping electron current pulse in plasma is presented. This scheme relies on the inhomogeneity of the plasma medium. This mechanism can be used for heating an overdense regime of plasma where lasers cannot penetrate. The method can ensure efficient localized heating at a desired location. The suitability of the scheme to the frontline fast ignition laser fusion experiment has been illustrated.

Keywords. Electron magnetohydrodynamics; fast ignition; collisionless stopping.

PACS Nos **52.30.Cv; 52.65.Kj; 52.57.Kk**

1. Introduction

Electrons can be easily accelerated to high energies because of their small mass-to-charge ratio, and hence are a good source of energy. They can be employed to heat overdense region of plasma medium where other energy sources such as laser field cannot penetrate. Since the accelerated high-energy electrons have to be injected from outside into the high-density plasma region for this purpose, the energetic electrons clearly needs to traverse through an inhomogeneous plasma medium. This highlights the importance of studying the propagation and transport characteristics of energetic electrons through inhomogeneous plasma medium, which is the topic of this paper. The electron transport through plasma medium occurs at fast time-scales, in which the heavier ions species can be assumed to be stationary, merely providing a neutralizing background. The description of electron magnetohydrodynamics (EMHD) model [1], therefore appears suitable for the depiction of the physics of electron transport.

The EMHD fluid model, however, considers evolution of a magnetized electron fluid through a homogeneous plasma. We have recently generalized the EMHD fluid model to the case when plasma density is inhomogeneous [2]. The salient features of this generalized EMHD (G-EMHD) model is presented in §2. In §3 we present simulation results obtained by evolving the G-EMHD set of equations which highlight the specific role of plasma density inhomogeneity, in the propagation of electron current pulses. The studies show that the electron current pulses can penetrate a high-density plasma region but are unable to move out again in regions where the plasma density is low. It is also observed that a sharp current shock forms at the density inhomogeneity layer while the electron pulse is entering a high-density plasma region. A rapid energy dissipation occurs at the current shock layer. The energy dissipation in shock structure forms the basis of collisionless stopping of electrons discussed in this paper. A quantitative understanding of the process of energy dissipation has also been provided.

High-energy electrons are essentially collisionless (Rutherford collision cross-section diminishes with energy). Therefore, if one only had to rely on classical Coulomb collisions for energy deposition, the electron energy has to be constrained at a low value. This in turn would affect the efficiency of the energy deposition process. The possibility of electron stopping by the process of their energy dissipation in shock structure removes this constraint and facilitates the use of electrons with higher energies. The presence of such an anomalous energy dissipation mechanism is therefore of great importance. Furthermore, studies show that since the mechanism is dependent on density inhomogeneity, by an appropriate tailoring of the inhomogeneity profile one can maneuver the location where one intends to deposit the energy. On the other hand, the collisional process does not provide one with such a freedom. In §4 we show the relevance of this density inhomogeneity-induced anomalous energy dissipation mechanism for the experimental case of fast ignition. Section 5 contains conclusion.

2. The G-EMHD model

The G-EMHD model is the generalization of the electron magnetohydrodynamic model (EMHD) for the case when the plasma density can vary in space. The electron fluid equations along with the relevant Maxwell's equations constitute the description of the model. The EMHD regime ignores the space-charge related effects and considers a magnetized electron fluid. Specifically, the time-scales of interest are assumed to be slower compared to the minimum value of the local plasma frequency ω_{pe} and/or $\omega_{pe}^2/\omega_{ce}$ (here ω_{ce} is the electron gyrofrequency) whichever is smaller. This ensures that the electron charge density fluctuations can be ignored and the electron continuity equation can be dropped. The Ampere's law also gets simplified as the displacement current can be dropped under this approximation. The EMHD model in the presence of plasma density inhomogeneity can be written in the normalized form as

$$\frac{\partial \vec{g}}{\partial t} = \nabla \times \left[\vec{v} \times \vec{g}\right], \tag{1}$$

$$\vec{v} = -\frac{1}{n}\nabla \times \vec{B}; \qquad \vec{g} = \frac{\nabla^2 \vec{B}}{n} - \nabla\left(\frac{1}{n}\right) \times (\nabla \times \vec{B}) - \vec{B}. \tag{2}$$

Here, g physically represents the generalized vorticity, containing contributions from both the field and the kinetic part. Furthermore, n, $\vec{B}$ and $\vec{v}$ denote plasma density (which is also the electron density in EMHD), magnetic field and electron velocity respectively in normalized units. The electron density has been normalized with the minimum value of the plasma density n_{00} in the region of interest, and the length by the skin depth $d_{e0} = c/\omega_{pe0}$ ($\omega_{pe0} = 4\pi n_{00} e^2/m_e$) corresponding to this density. The magnetic field is normalized by B_0, the typical magnitude of the magnetic field and the time by the corresponding electron gyrofrequency $\omega_{ce0} = eB_0/m_e c$. When variations are confined in 2D $x-y$ plane, the G-EMHD model can be written as a coupled set of equations for two scalar fields b and ψ.

$$\frac{\partial}{\partial t}\left\{b - \nabla\cdot\left(\frac{\nabla b}{n}\right)\right\} + \hat{z}\times\nabla b\cdot\nabla\left[\frac{1}{n}\left\{b - \nabla\cdot\left(\frac{\nabla b}{n}\right)\right\}\right] + \hat{z}\times\nabla\psi\cdot\nabla\left(\frac{\nabla^2\psi}{n}\right) = 0 \quad (3)$$

$$\frac{\partial}{\partial t}\left\{\psi - \frac{\nabla^2\psi}{n}\right\} + \frac{\hat{z}\times\nabla b}{n}\cdot\nabla\left\{\psi - \frac{\nabla^2\psi}{n}\right\} = 0. \quad (4)$$

Here b and ψ respectively represent the magnetic field and the vector potential component along the symmetry direction $\hat{z}$. Thus $\vec{B} = b\hat{z} + \hat{z}\times\nabla\psi$. The G-EMHD evolution can be further simplified when the electron current is constrained in the 2D $x-y$ plane of variation. For this case $\psi = 0$ making eq. (4) irrelevant. We present here results for this particular case. However, it has been verified that the same conclusions hold for the general case, when both b and ψ are finite.

3. Electron current propagation through inhomogeneous plasma density

We wish to understand how the density inhomogeneity influences the evolution of electron current pulses. For this purpose we isolate the effect of density inhomogeneity on the electron current pulse propagation by choosing exact nonlinear solutions of the EMHD equations (the homogeneous plasma case) as initial condition. The exact nonlinear solutions of EMHD are of two types [3]. One has monopolar magnetic fields, which are the solutions of the equation $\nabla^2 b = F(b)$ (where F is any function of b). These solutions are stationary rotating currents in a homogeneous plasma and acquire a drift velocity of $V_n = (\hat{z}b\times\nabla n)/n^2$ in the presence of inhomogeneity. The other one has the dipolar magnetic field structures which are the solution of $\nabla^2 b - b = F(b - Ux)$ and propagate undistorted with a velocity U along their axes in a homogeneous plasma. The axial speed U is high for those solutions which have their lobes closer, and the associated magnitude of the magnetic field b is high. The interesting aspect of these dipole solutions is that the current pattern associated with them mocks up spatially separated (through Weibel instability) forward (externally injected electrons) and return shielding current (offered by background plasma).

When such a dipole structure encounters a density inhomogeneity, in addition to its intrinsic axial propagation speed it also acquires a drift velocity of $V_n = (\hat{z}b\times\nabla n)/n^2$ [2]. The interplay of these two kinds of drifts then produces a host of interesting features. We report some observations here which are relevant in the context of electron energy dissipation.

In figures 1 and 2 we show the propagation of dipolar current pulse structures through a density cavity and a density hump respectively. This drift V_n is opposite for the two lobes, the sign of b being different for the two lobes. The combination of the axial and the V_n drift (which is distinct for the two lobes) decides the subsequent evolution of the structure. In figure 1 it is shown that the dipole is unable to enter a low-density cavity (indicated by the black circular lines) it encounters in its path. The two lobes separate, due to their respective V_n drift and after circling around the lower density cavity region again join to form a dipole and propagate forward. On the other hand, when the dipole encounters an increasing plasma density as shown in figure 2 it readily enters the region of high density. However, once inside the high-density region it is unable to come out from there. The central circular region in figure 2 has a 10 times higher density than the background outer region. In this case since the density gradient has a reverse configuration compared to that of figure 1, the V_n drift associated with the two lobes brings the lobes closer when the structure encounters a density hump. As a result, the axial speed U increases and the dipole enters the high-density region very rapidly. When the structure reaches the other end of the circular density hump it is observed that the lobes separate. This happens as the associated V_n separates the two lobes, thereby, reducing U. In fact, once the lobe separation is larger than the electron skin depth, the two lobes act as individual monopoles and drift along the circular boundaries of the density hump. The lobes again join and traverse along the diameter of the cavity as a dipole. This prcoess repeats and the dipolar structure remains trapped inside the

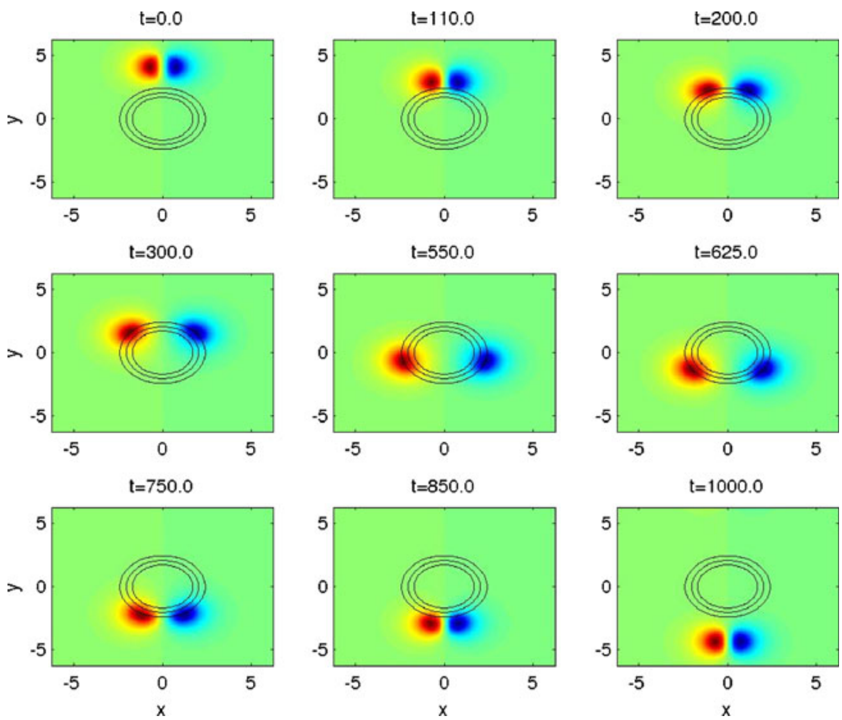

Figure 1. Propagation of dipole as it encounters a density cavity.

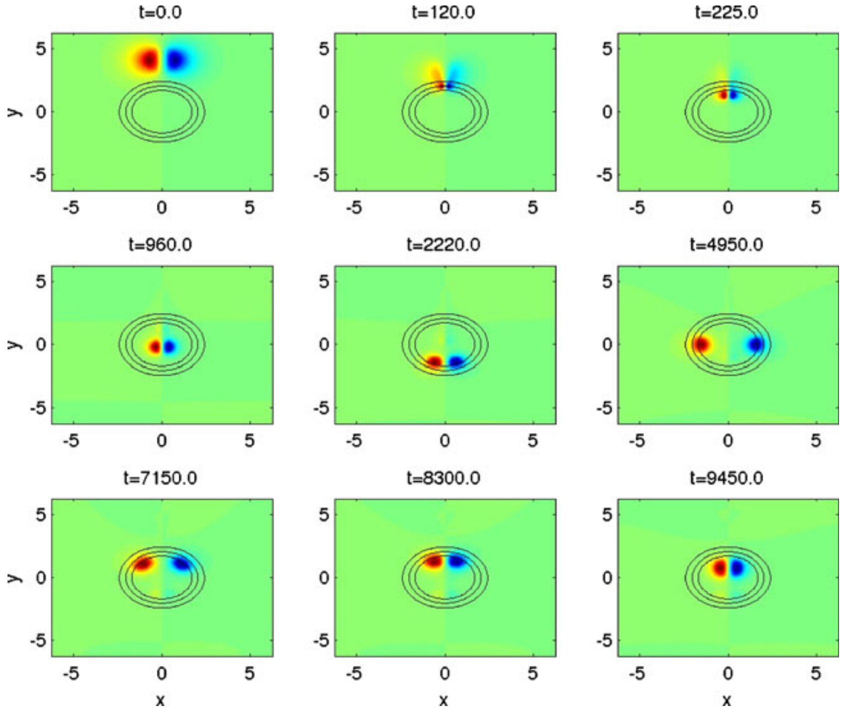

Figure 2. Propagation of dipole as it encounters a density hump.

density hump. At times, for some configurations, the structures have been observed to get transmitted out of a high-density region. A systematic study using various density profiles and various dipolar solutions shows that (i) the behaviour of transmission vs. trapping is independent of the properties of the chosen dipole solution, (ii) it is also independent of the value of maximum density in the density profile, (iii) the density gradient, as expected, is found to be responsible for trapping, (iv) there exists a threshold value of $L_n/L = \alpha_{\mathrm{T}}$ (density gradient scale length/propagation distance in the inhomogeneous layer) above which the structure gets transmitted and below which the structure is trapped. It should be noted that the trapping of current pulse structures in a high-density plasma region can be looked upon as a simple mechanism for plasma-based tweezer for electron currents.

The trapping of the current pulse structure in the high-density region is clearly a violation of time reversal invariance and is suggestive of a dissipative process at work. This is indeed corroborated by studying the evolution of total energy which shows a sudden drop at the time when the structure moves past the inhomogeneity layer while entering the high-density region. The mechanism of this sudden energy dissipation can be traced to the current layer shock formation due to the collision between the two lobes of the dipoles as they move with their respective V_n drifts. This shock is also captured in the simulation of inertialess limit of the G-EMHD equation. The analytical understanding of the shock formation can be gleaned by considering the inertialess limit of the G-EMHD equation, which can be cast in the form of Burger's equation.

When the terms related to the electron inertia are dropped from the G-EMHD equation, the evolution equation can be cast as

$$\frac{\partial b}{\partial t} + \hat{z} \times \nabla b \cdot \nabla \left\{ \frac{b}{n} \right\} = \eta \nabla^2 b - \mu \nabla^4 b. \tag{5}$$

In the above equation we have specifically introduced the resistivity and viscosity coefficients. The case in which these coefficients tend towards zero is also included in our analysis. The evolution of inertialess case through eq. (5) has shown that in this case though the dipoles do not move axially they continue to drift due to V_n and the shock structure develops. Taking $\hat{y}$ as the direction of density inhomogeneity, the magnetic field is along $\hat{z}$ and V_n is directed along x. The shock structure, therefore, develops along x. Since the structure possesses sharp variation along x we retain only the x derivatives of eq. (5) to obtain

$$\frac{\partial b}{\partial t} + Kb \frac{\partial b}{\partial x} = \eta \frac{\partial^2 b}{\partial x^2} - \mu \frac{\partial^4 b}{\partial x^4}. \tag{6}$$

Here, $K = \partial / \partial y (1/n) = -1/L_n$ is the inverse of the density scale length. For a uniform K, eq. (6) is the Burger's equation which supports shock structure. In the stationary state the shock width is determined by the balance of the dominating dissipative term with the nonlinear term. In the two cases where either η or μ dominates, the shock width x_W can be shown to scales as (η/Kb) or $(\mu/Kb)^{1/3}$. The total dissipated energy for the resistive case can be written as

$$Q \sim \int \left[\eta \left(\frac{\partial b}{\partial x} \right)^2 \right] \mathrm{d}x L_z L \sim \eta \frac{b^2}{x_W} L_z L \sim KLL_z b^3. \tag{7}$$

Here, L and L_z are the typical distance traversed in the inhomogeneity layer and the typical extent of the structure along the symmetry direction. It should be noted here, that the total dissipated energy is independent of the value of η. When viscosity dominates, again the scaling of shock width is such that the dissipated energy

$$Q \sim \int \left[\mu \left(\frac{\partial^2 b}{\partial x^2} \right)^2 \right] \mathrm{d}x L_z L \sim \mu \frac{b^2}{x_W^3} L_z L \sim KLL_z b^3 \tag{8}$$

is the same as the resistive case, and hence again independent of both η and μ. Using Ampere's law we can express b in terms of the typical incoming current filament dimension a and the electron velocity u. Thus $b \sim au$. This shows that

$$Q \sim KLb^2 a L_z u \sim (L/L_n) a L_z u. \tag{9}$$

The energy dissipation depends on the same parameter ratio (L_n/L) which determined the criteria for trapping vs. transmission, noted earlier. Thus, when the dissipated energy is high for small L_n/L, the structure remains trapped inside the high-density region. In the other case, since the dissipated energy is small, the structure is transmitted past the inhomogeneous density hump as demanded by the time-reversal criteria.

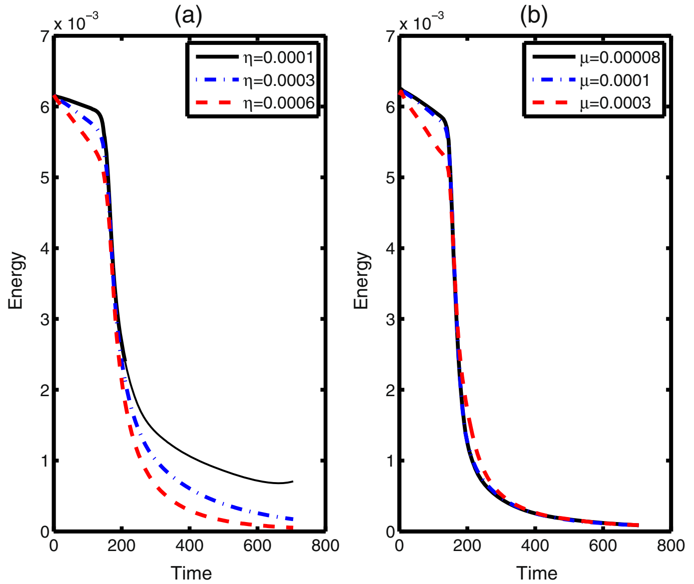

Figure 3. Evolution of total electron energy for various values of the (**a**) resistivity parameter η and (**b**) viscosity. The sudden decrease occurs at the time the pulse crosses the density inhomogeneity layer. The typical magnitude of this rapid dissipation is similar in all the cases.

Thus, sharper the density gradient and longer the distance traversed in the inhomogeneous region, higher is the amount of energy dissipated. Furthermore, the estimated energy dissipation is essentially equal to the entire incoming magnetic energy for $L = L_n$. For highly energetic electrons, the resistive damping could be weak. In this limit of vanishing resistivity, the anomalous viscous effects would spontaneously arise from the Kelvin–Helmholtz destabilization of the sharp current layers formed in the shock region and would dominate [5]. The dominant character of energy dissipation would change from resistive to that dependent upon the anomalous viscosity effects of the system, as the energy of the incident electrons increases. However, the total magnitude of the energy dissipated from these electrons remains insensitive to this change [4]. The G-EMHD simulations also illustrate this. The magnitude of total energy dissipation typically is of the same order even though the resistivity and viscosity parameters are chosen to be different for the various simulations shown in figure 3.

4. Application to fast ignition

This process of collisionless dissipation of electron energy has direct relevance to the fast ignition (FI) experiments [6]. The FI scheme is a simple variant of the inertial confinement fusion (ICF) technique. In FI the fusion target is compressed by a slow nanosecond pulse and then a separate fast sub-picosecond laser pulse is employed for the creation of hot spark. This has several advantages, the compression is easier and one no longer needs stringent spherical symmetry of the target and/or drive pressure as the hydrodynamic instabilities arising due to the assymetries are inconsequential. The femtosecond laser, however, cannot penetrate the overdense target region. One relies on the energetic electrons generated at the critical density region to propagate towards the compressed core and deposit their energy for the creation of ignition spark. Some scaled-down experiments [7] have shown FI to produce promising results with ten-fold increase in fusion events relative to the same experiment without employing the ignitor pulse. However, skepticism still prevails as one would require 1−3 MeV or even higher energy electrons for heating in the full-scale experiments. The classical stopping distance for 1−3 MeV electrons even after considering correlated collisions in the dense plasma environment turns out to be around 100−1000 microns, much longer than the compressed target size of 50 microns. The success of FI thus requires some collective plasma process to enhance the stopping efficiency. The collisionless energy dissipation process outlined in this paper provides the relevant collective process.

A strong evidence in support of such a collective process at work is provided by a recent experiment conducted at ILE Osaka [8]. The experiment measured electron energy spectrum with the help of two electron spectrometers placed at 20° and 40° angles with respect to the ignitor laser pulse axis on the opposite side of the target. The electrons collected by the 20° ESM have to pass through the compressed plasma core region and hence traverses the inhomogeneous plasma density, whereas the ESM at 40° collects electrons passing through the low coronal density region of the target. The ultra intense laser (UIL) was sent at various distinct time with respect to the maximum compression timing. It is observed that while there is hardly any difference in the electron energy spectrum for the 40° ESM, the ESM at 20° registers a marked drop in the number of electrons having energy as high as 15 MeV when the UIL pulse timing properly coincides with the timing of the compression pulse. The stopping of the 15 MeV electrons can also be understood. We had noted that the energy dissipation typically is of the order of the incoming magnetic energy associated with the current pulse. In non-dimensional form, this translates to

$$B = \frac{2I}{ac}; \qquad Q \sim \frac{B^2}{4\pi}\pi a^2 c = \frac{I^2}{c} = I^2 R. \tag{10}$$

This expression shows that the effective resistivity $R = 1/c = 30\ \Omega$. The current associated with the electrons in the experiment is measured to be around 0.5 Mega Amperes. One can thus expect a voltage drop of $IR = 15$ Mega Volts which will stop electrons with 15 MeV energy. Thus the estimates based on our analysis provide good quantitative agreement. Another strong evidence in support of the mechanism comes from the published PIC simulation data which show that in all studies the heating occurs at a location where the density inhomogeneity is maximum. We thus observe that the existence of anomalous collisionless scheme of energy dissipation helps us to extract energy from those high-energy electrons which otherwise would have propagated unhindered. This helps in increasing the heating efficiency. It should also be noted that the location of plasma heating can be maneuvered by an appropriate tailoring of the plasma density profile.

In addition, it is also desirable for efficient plasma heating at a localized spot that the electron beam spreading during the course of its propagation be minimum. Several schemes have been proposed in the past to collimate and guide the electrons. One of them is the use of specially structured targets made of different materials [9]. Such targets would neither be easy to prepare nor can they be employed in each and every experiment. An easier accessable scheme is therefore desirable. Our preliminary simulation studies show that a properly tailored plasma density offers such a possibility. The results on collimating and guiding electron current pulse structures will be reported elsewhere.

5. Conclusion

Electrons can be a good source of energy for heating plasma. This is specially important as they can penetrate a high-density overdense region which are not accessable by laser fields. The study of electron transport through plasma is, therefore, an important area for investigative purposes. We propose a collisionless energy dissipation scheme based on the current shock formation at the inhomogeneous plasma layer. In FI scheme thus high-energy collisionless electrons can be employed for creating ignition spark. The ILE experiment and the published PIC data support the proposed mechanism.

Acknowledgement

AD would like to acknowledge the support of her DAE-SRC (Department of Atomic Energy Science Research Council) grant (Sanction No. 2005/21/7-BRNS/2454) for this work.

References

[1] A S Kingsep, K V Chukbar and V V Yankov, *Reviews of plasma physics* (Consultant Bureau, New York, 1990) Vol. 16 and references therein
[2] S K Yadav, A Das and P Kaw, *Phys. Plasmas* **15**, 062308 (2008)
[3] M B Isichenko and A M Marnachev, *Sov. Phys. JETP* **66**, 702 (1987)
[4] S K Yadav, A Das, P Kaw and S Sengupta, *Phys. Plasmas* **16**, 040701 (2009)
[5] A Das and P Kaw, *Phys. Plasmas* **8**, 4518 (2001)
N Jain, A Das, P Kaw and S Sengupta, *Phys. Lett.* **A363**, 125 (2007)
[6] M Tabak, I Hammer, M E Glinsky *et al*, *Phys. Plasmas* **1**, 1626 (1994)
[7] M H Key *et al*, *Nature* **412**, 775 (2001)
R Kodama *et al*, *Nature* **412**, 798 (2001)
R Kodama *et al*, *Nature* **418**, 933 (2000)
[8] T Yabuuchi, A Das, G R Kumar, H Habara, P K Kaw, R Kodama, K Mima, P A Norreys, S Sengupta and K A Tanaka, *New J. Phys*. **11**, 093031 (2009)
[9] S Kar, A P L Robinson, D C Caroll, O Lundh, K Markey, P McKenna, P Norreys and M Zepf, *Phys. Rev. Lett*. **102**, 055001 (2009)